PRE-STROKE RADIATION FROM THUNDERCLOUDS

by

Kenneth Lee Zonge

A Thesis Submitted to the Faculty of the

DEPARTMENT OF ELECTRICAL ENGINEERING

In Partial Fulfillment of the Requirements
For the Degree of

MASTER OF SCIENCE

In the Graduate College

THE UNIVERSITY OF ARIZONA

1 9 6 5

STATEMENT BY AUTHOR

This thesis has been submitted in partial fulfillment of requirements for an advanced degree at The University of Arizona and is deposited in the University Library to be made available to borrowers under rules of the Library.

Brief quotations from this thesis are allowable without special permission, provided that accurate acknowledgment of source is made. Requests for permission for extended quotation from or reproduction of this manuscript in whole or in part may be granted by the head of the major department or the Dean of the Graduate College when in his judgment the proposed use of the material is in the interests of scholarship. In all other instances, however, permission must be obtained from the author.

SIGNED: Kenneth L. Zonge

APPROVAL BY THESIS DIRECTOR

This thesis has been approved on the date shown below:

W. H. Evans — April 28, 1965

W. H. EVANS
Professor of Electrical Engineering

Date

ACKNOWLEDGEMENTS

The author is pleased to thank Professor W. H. Evans for his interest and guidance throughout the course of this work, and the staff of the Applied Research Laboratory whose assistance made the completion of this work possible.

The author wishes to thank the National Science Foundation whose support through Research Grant GP-800 made this study possible.

The author also thanks his wife for her understanding and patience which made this study a more pleasant task.

TABLE OF CONTENTS

LIST OF ILLUSTRATIONS

LIST OF TABLES

ABSTRACT

This thesis is concerned with the experimental determination of electromagnetic noise emission from a thundercloud from the beginning of internal charge build-up until, but not including, the occurrence of major discharges.

The experimental apparatus and procedure used for the measurement of the noise emission are explained in detail, and results are given for 12 kc, 100 kc, 2.5 Mc, 10 Mc, and 110 Mc.

This study was made possible through National Science Foundation Research Grant GP-800.

Chapter 1

INTRODUCTION

1.1 The Problem and Justification

A need to detect the initial electrical activity in cumulus clouds and to locate storm cells having a high probability of giving cloud-to-cloud or cloud-to-ground discharges prompted this research.

Presently, at The University of Arizona, several projects are being conducted which depend on the accurate location and photographic recording of lightning discharges. These photographic records are obtained by positioning a camera or spectrograph in the general direction of a storm cell which visually appears most likely to be active and to produce the needed discharges. If a method could be devised which would ferret out the active cells that are approaching discharge capacity, one could increase the percentage of strokes recorded and thus enhance the quantity of usable data in this area. Therefore, if a storm tracking apparatus utilizing radio frequency emission from the thunderstorm cells could be fabricated, one could either mount on the tracking antenna, or slave to it, the necessary apparatus for scientific photographic recording. Also, at the same time it is hoped that more can be learned about the static charge build-up within a thundercloud. Hence, a project was initiated to see if there is indeed any appreciable pre-stroke radiation and to determine if it could be applied toward storm tracking and toward furthering the knowledge of storm cell charge build-up.

1.2 Approach

It was decided to construct and operate equipment on a logarithmic frequency scale in order to cover a large portion of the frequency spectrum and obtain a good measure of the frequency distribution of the emission. Consequently, antennas and receiving systems were either constructed or obtained for 12 kc, 100 kc, 2.5 Mc, 10 Mc, 110 Mc, and 1 Gc, where the deviations from the logarithmic frequency scale are due to local interfering signals. Good data was obtained on the lower four frequencies, with an indication of radio frequency emission on 110 Mc, and no results on 1 Gc. The lack of data on the two higher frequencies is attributed to lack of proper receiver sensitivity.

Since this experiment is concerned with long term (minutes) noise variance, the detected signal was smoothed by an RC network with approximately a two second time constant and then mechanically integrated over a one minute period every 15 minutes. This information was then plotted on graph paper for analysis. The good data was then reanalyzed after reducing the spacing between integration periods to five minutes.

Chapter 2

THEORY

2.1 Expected Radiation

Jansky[1] was one of the first investigators of atmospheric noise. With a rotating array he obtained data which indicated the presence of three different groups of static: static from local thunderstorms; static from distant thunderstorms; and static of an unknown origin which was later found to be from cosmic sources.

One should expect radiation of some nature from a thunderstorm cell if only by virtue of the large electrostatic fields present within such a cell causing local glow currents. With the continual convection air currents, charge build-up and movement, and finite conductivities within a cell, it seems reasonable to expect minor internal arcing, discharging, or corona, any one of which would produce radiation. Sartor[2] indicates that electromagnetic emission from thunderclouds may come from a large number of charged water drops colliding and has observed radiation in the 25 to 30 Mc region experimentally. Hogg and Semplak[3] have observed 5 cm (6 Gc) noise emission from convective clouds which increased the sky noise temperature as much as 17 db.

However, in this work simultaneous increases on frequencies from 12 kc to 10 Mc were noticed which tends to indicate noise sources due to different parameters. Along this line, Large[4] experimentally determined that corona from conductors near his receiving antenna produced a continuous noise voltage which is proportional to the reciprocal of the

frequency from 100 kc to 10 Mc. Sayers, Forrest and Lane[5] have observed similar interference from a test high voltage power line.

Many authors have conducted experiments concerning radio frequency emission in the very low to very high frequency range from lightning strokes. Aiya[6,7] indicates that the main source of noise in the 1 to 20 Mc region from tropical storms is due to the stepped leader in discharges within a cloud and the noise radiated below 1 Mc is due to the stepped leader in discharges from cloud-to-ground. Using low frequency data, Aiya makes assumptions about the variations of discharge currents in a stepped leader and theoretically deduces that noise power in the 1 to 20 Mc region is proportional to the inverse square of the frequency.

Contrary to Aiya's results, Horner[8] found that the stepped leader contributed only a small part of the noise at 11 Mc and the main sources could not be quantitatively identified with any of the presently known processes of the lightning discharge. Moreover, Horner found that at 6 kc the largest pulses in most of the atmospherics could be attributed to the return strokes, and some of the smaller pulses appeared to be from discharges within the cloud which exhibited characteristics similar to those of return strokes.

Hill[9] has made a theoretical investigation of radiation from lightning strokes at very low frequencies and concludes that the form of the spectral distribution is determined by the time of travel of the return stroke. Using this parameter, Hill predicts radiation in the megacycle region which approximately agrees with Aiya.

Arnold and Pierce[10] and Dennis and Pierce[11] have recently given

a detailed analysis showing that substantial radiation at very low frequencies originates in the leader and junction processes of the lightning discharge, as well as the return stroke, although to a lesser degree. Pierce[13] indicates that the dominant noise at high frequencies may be due to filimentary sparks from advancing streamers and, to a much lesser degree, corona from the lightning channel. Therefore, although one does not have general agreement as to the originating processes for atmospherics in all frequency ranges, it is generally conceded that the lightning process produces radio frequency noise in the very low to high frequency region. It is reasonable then to suspect that pre-stroke radiation from thunderclouds could originate from intercloud corona, from internal arcing, or from discharges similar to the leader processes.

2.2. Averaging and Weighting Functions

The effect of bandwidth on various types of noise has been investigated by Landon[13] and Jansky[14]. They found that for atmospheric noise (i.e. noise characterized by a large number of overlapping pulses) the peak, average, and effective voltages are proportional to the square root of the bandwidth. Therefore, the data obtained in this experiment is normalized to the square root of the bandwidth in kilocycles.

The equivalent noise bandwidth was measured by mechanically integrating a plot of the square of the voltage response of each receiver at the frequency recorded. The relationship used was

$$BW_{equiv} = \frac{\int_0^\infty A^2 \, df}{A_0^2}$$

where A = the voltage amplification at frequency f and A_o is the maximum voltage amplification occuring at the center frequency f_o. The bandwidth referred to throughout the text is the equivalent noise bandwidth.

The recorded data was reduced by calculating the average voltage over a one minute period (T). The average voltage is taken as

$$E_{av} = \frac{1}{T} \int_0^T e(t)\, dt$$

This parameter was obtained by mechanically integrating the chart recordings with a planimeter and dividing by the period.

Chapter 3

THE EXPERIMENTAL SETUP

3.1 Location

The experimental site (Figs. 3.1 and 3.2) is located on land of the USCGS Magnetic Observatory approximately 13 miles northeast of Tucson, Arizona. This site was picked because of its accessibility and relative low noise surroundings.

3.2 Antennas and Preamplifiers

The antennas used are shown in Figs. 3.3, 3.4, 3.5, and 3.6. The buried ground system of the antennas for 100 kc, 2.5 Mc, and 10 Mc consists of 36 radials of number 10 copper wire each 50 feet long and tied together about the periphery. Six foot ground rods were driven at the center of the array and at the end of every sixth radial.

The antennas for 12 kc, 100 kc, and 2.5 Mc are matched at the base by a cathode follower system and the 12 kc and 100 kc signals are also preamplified at this point. The signals are then fed into the receiving house for further amplification and detection. Table 3.1 describes the antenna systems.

3.3 Receivers and Recording System

Shop-made receivers were utilized on 12 kc and 100 kc; modified Hammerlund Model Sp-600 receivers on 2.5 Mc and 10 Mc; and modified army radar search receivers, Model APR-4, on 110 Mc and 1 Gc. All signals were linearly detected and then passed through RC smoothing filters.

Fig. 3.1 Experimental Site

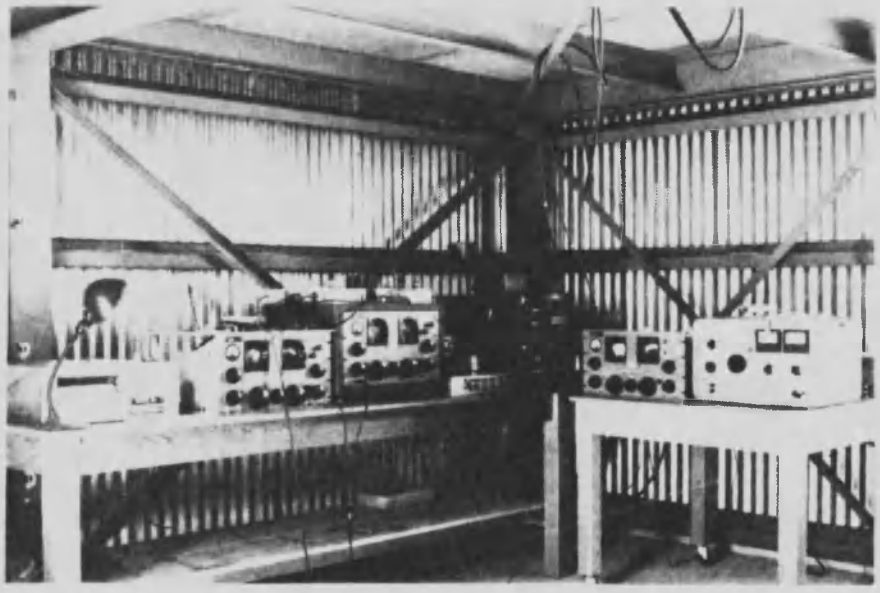

Fig. 3.2 Equipment used for Receiving and Recording Noise Signals.

Fig. 3.3 12 kc Antenna

Fig. 3.4 100 kc and 2.5 Mc Antenna

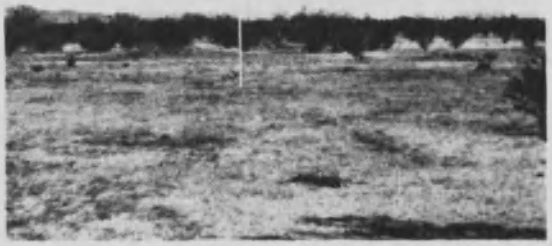

Fig. 3.5 10 Mc Antenna

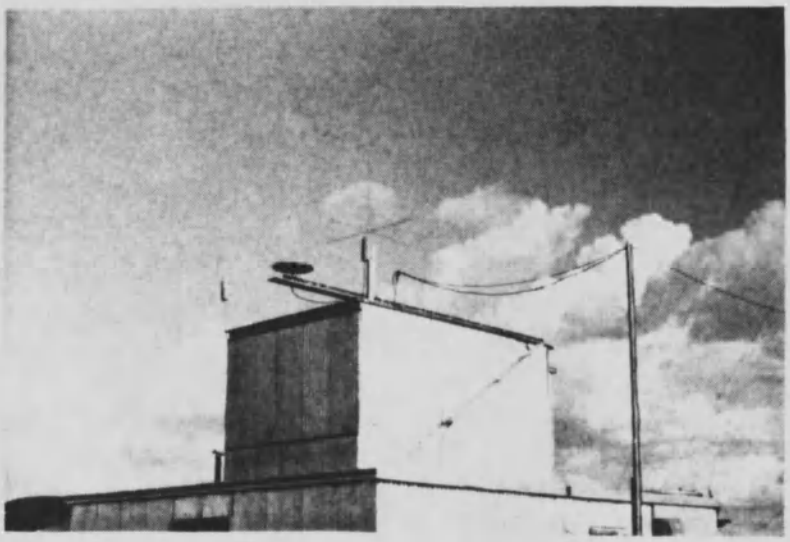

Fig. 3.6 110 Mc and 1 Gc Antennas

Table 3.1 Antenna Parameters

Frequency	Antenna Type	Physical Height	Effective Height	Approximate Input Impedance
12 kc	Ground Plane (Incremental Monopole)	1 m	1/2 m	$-j8.28 \times 10^{+5}$ (16 $\mu\mu$f)
100 kc	Vertical	8.85 m	4.4 m	1.7×10^{-8} $-j2.0 \times 10^{+4}$ (79 $\mu\mu$f)
2.5 Mc	Vertical	8.85 m	4.4 m	2.2 -j747 (85 $\mu\mu$f)
10 Mc	Vertical 1/4 λ Monopole	7.125 m	4.5 m	30 Ω
110 Mc	Ground Plane 1/4 λ Folded Monopole	0.615 m	0.39 m	95 Ω
1 Gc	Ground Plane 1/4 λ Folded Monopole			

Measured time constants of these filters and equivalent noise bandwidths of the receivers are given in Table 3.2, and a block diagram of the entire system is shown in Fig. 3.7.

From the filters the signals were fed into a Honeywell Model 1508 Visicorder Oscillograph which made a simultaneous, continuous recording of the six channels at a constant chart drive of 0.1" per second. The charts were then permanized for analysis.

3.4 Calibration

All channels were calibrated through an equivalent dummy antenna with an unmodulated sine wave. The channels were calibrated two times a week and were checked approximately once an hour during the recording period for zero drift.

3.5 Supporting Equipment

Throughout a majority of the data recording days, continuous field mill records were obtained. These records proved valuable in correlating the noise recordings with nearby cloud movement and such phenomena as point discharge from the antennas and cloud and ground discharges.

A Model APS-23 X-band radar was utilized to detect storm cells which contained particles large enough for a radar return (approximately 200 microns in diameter) as well as those cells which were already electrically active or in the precipitation stage. Thus the radar aided visual observations and the logging of sky conditions during the noise recordings.

Table 3.2 Receiver Characteristics

Frequency	Time Constants	Equivalent Noise Bandwidth
12 kc	Charge 2.6 sec Discharge 3.8 sec	0.39 kc
100 kc	Charge 2.8 sec Discharge 3.5 sec	4.1 kc
2.5 Mc	Charge 1.9 sec Discharge 2.0 sec	8.5 kc
10 Mc	Charge 1.9 sec Discharge 1.9 sec	8.1 kc
110 Mc	Charge 0.19 sec Discharge 0.22 sec	1050 kc

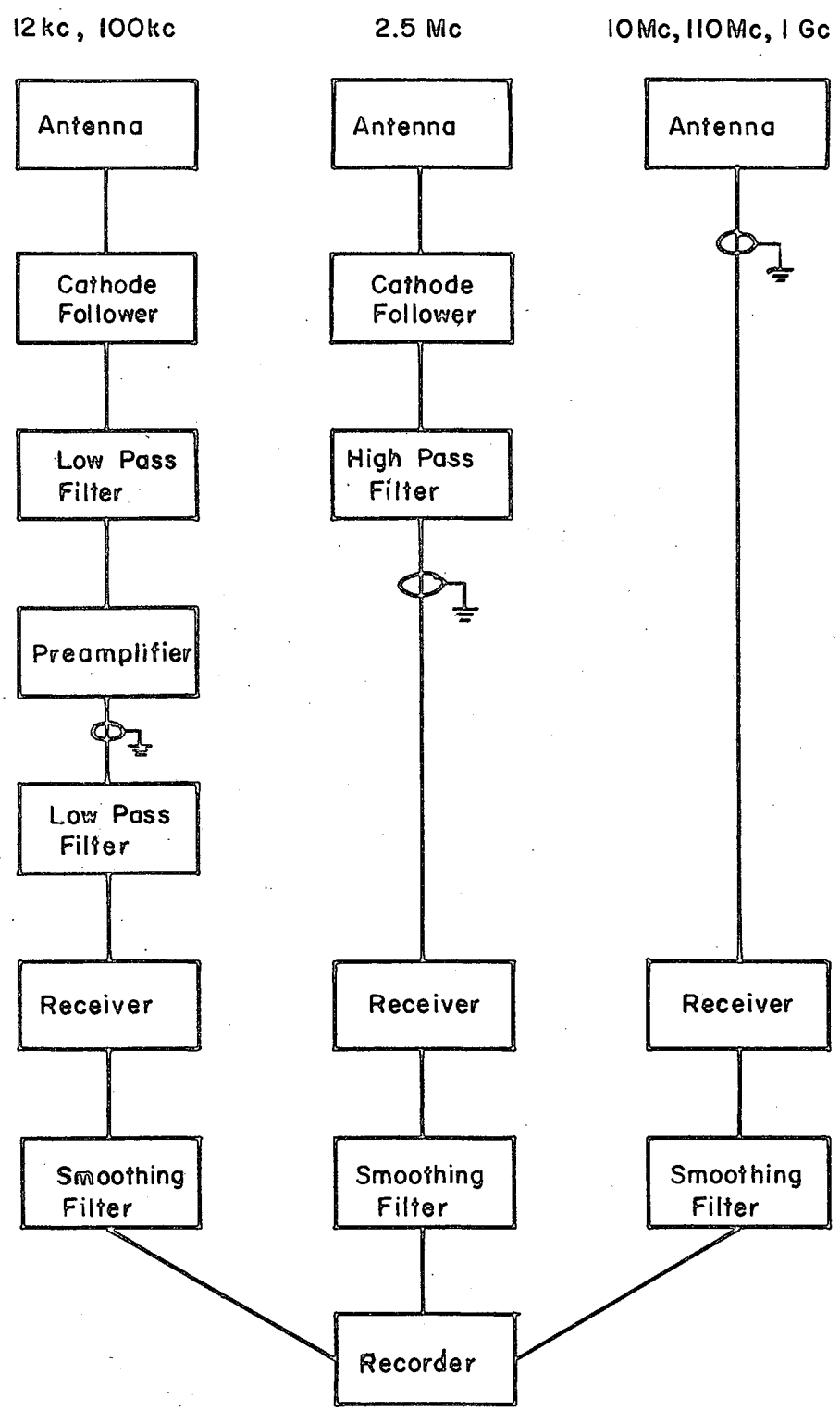

Fig. 3.7 Block Diagram of Noise Receiving and Recording System.

Chapter 4

Analysis of Records

4.1 Initial Stage

Initial analysis consisted of inspecting the noise voltage recordings every 15 minutes, recording the average noise voltage at that time, and plotting the results for comparison. Then these noise plots, with the daily log and the field mill records were inspected for variations and patterns which might tend to indicate storm cell build-up, activity, or movement. A sample of the noise voltage chart recording is given in Fig. 4.1.

4.2 Final Stage

Excellent correlation between pre-stroke radiation and storm cell build-up was obtained on August 27, 1964. Between 2:00 and 3:00 PM an isolated storm cell was observed to move from a position 14 miles northeast of the observation site to within 9 miles and then move away from the site to end up directly east at 14 miles where it eventually dissipated. During the lifetime of the cell it produced two ground strokes, both of which were observed visually, on the field mill records, and on the noise recording. These records were used as a guide to analyze other noise data, since such good correlation was obtained on this storm and it was one of the few isolated cells which formed during the summer.

It was noted that during this storm the noise radiation peaks seldom exceeded 100% of the average minimum value during a one minute period except for radiation from major discharges. Therefore, it was

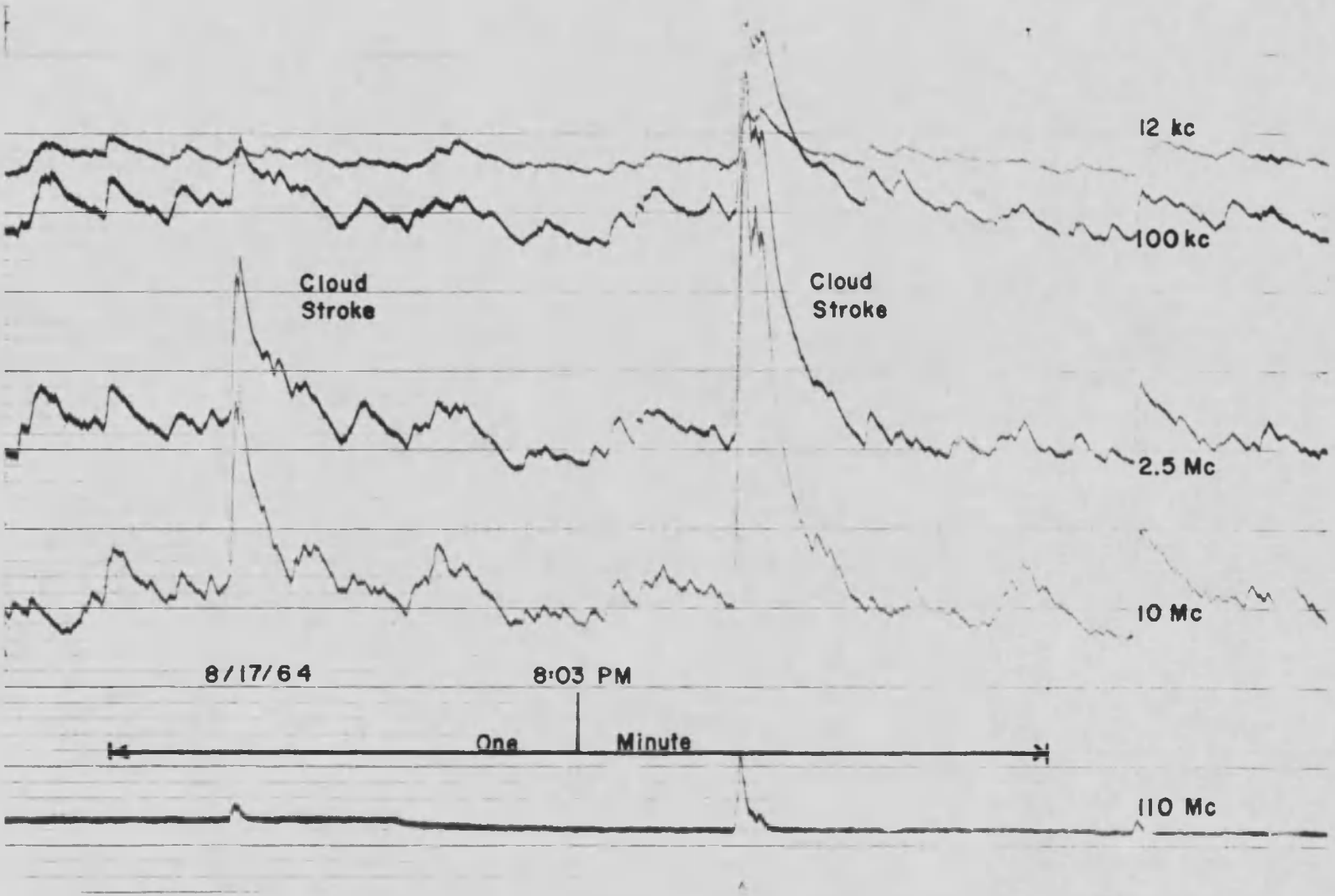

Figure 4.1 Sample of the Noise Voltage Chart Recording

decided to clip all voltage peaks which exceeded 100% of the average minimum value in an effort to obtain a better measure of the average noise build-up.

The records which were chosen through the initial analysis were re-integrated over a one minute period every five minutes and plotted. From these plots, the data which definitely showed an increase in noise radiation during storm build-up was analyzed. Only one day other than August 27 gave definite results. This was August 24, 1964, on which day a single storm cell was observed 17 miles north of the observation site at 2:50 PM. The storm stayed in this general area during the observation time and by 3:40 PM had broken up into three cells which ranged from 12 to 15 miles north and northeast of the site. No strokes from the storm cell were noted visually since a mountain range was between the storm cell and the observation point. Therefore, the stroke data was extracted from the field mill records.

The lack of additional data is attributed to the use of non-directional antennas since during most of the stormy days there were so many different storms in the general area that the effect of any one cell was masked out by the others.

Figures 4.2 and 4.3 are composites of sections of noise recordings for storm A (August 24) and storm B (August 27) respectfully. The change in background noise can be seen from these sequences. There is a definite change in noise structure as the storm grows in intensity. The structure changes from a low level, almost continuous background noise with large, widely spaced, discrete pulses to a high level background composed of continuous noise and closely spaced discrete pulses with

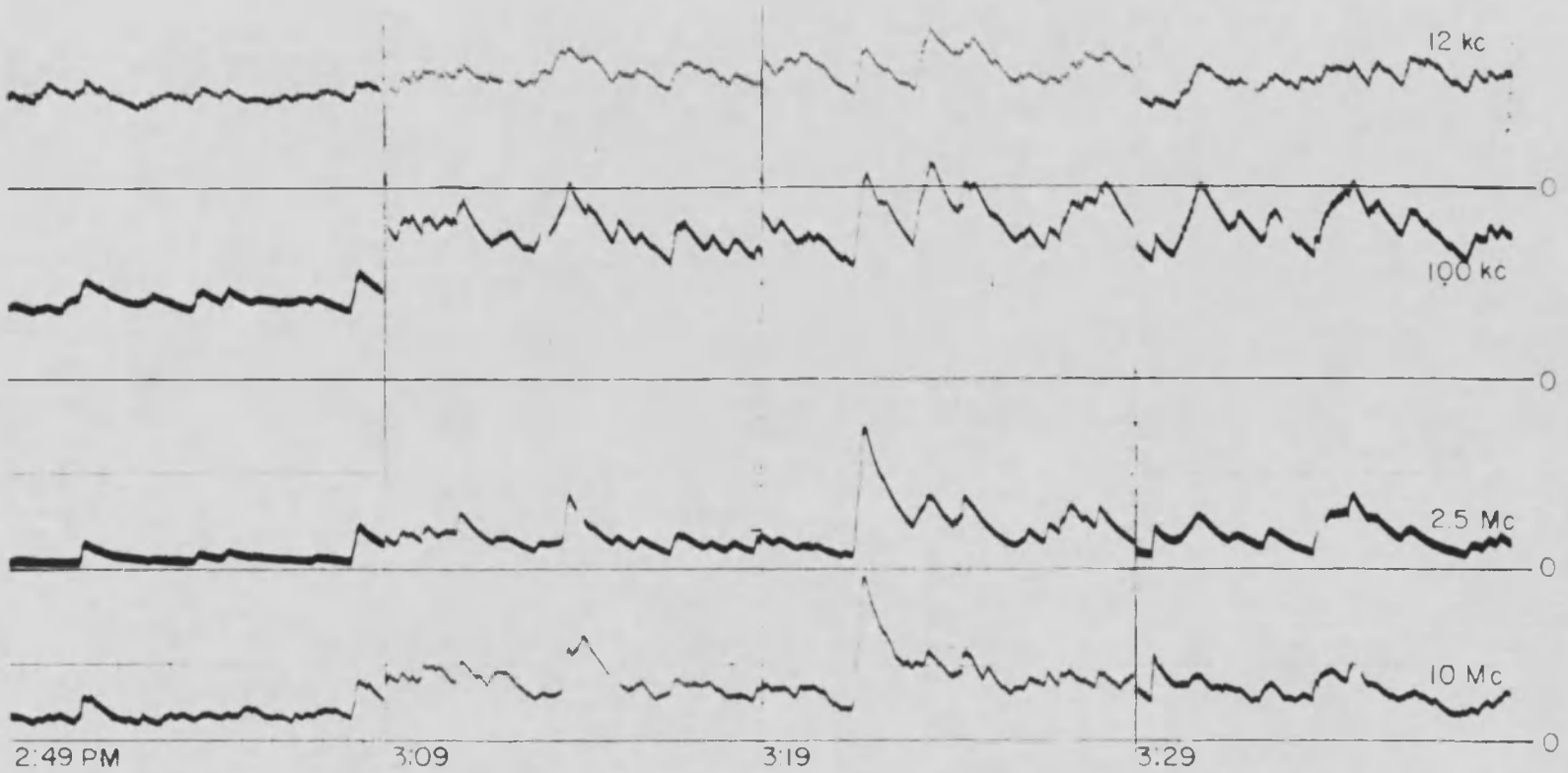

Fig. 4.2 Composite of Sections of Noise Recording for Storm A (August 24, 1964)

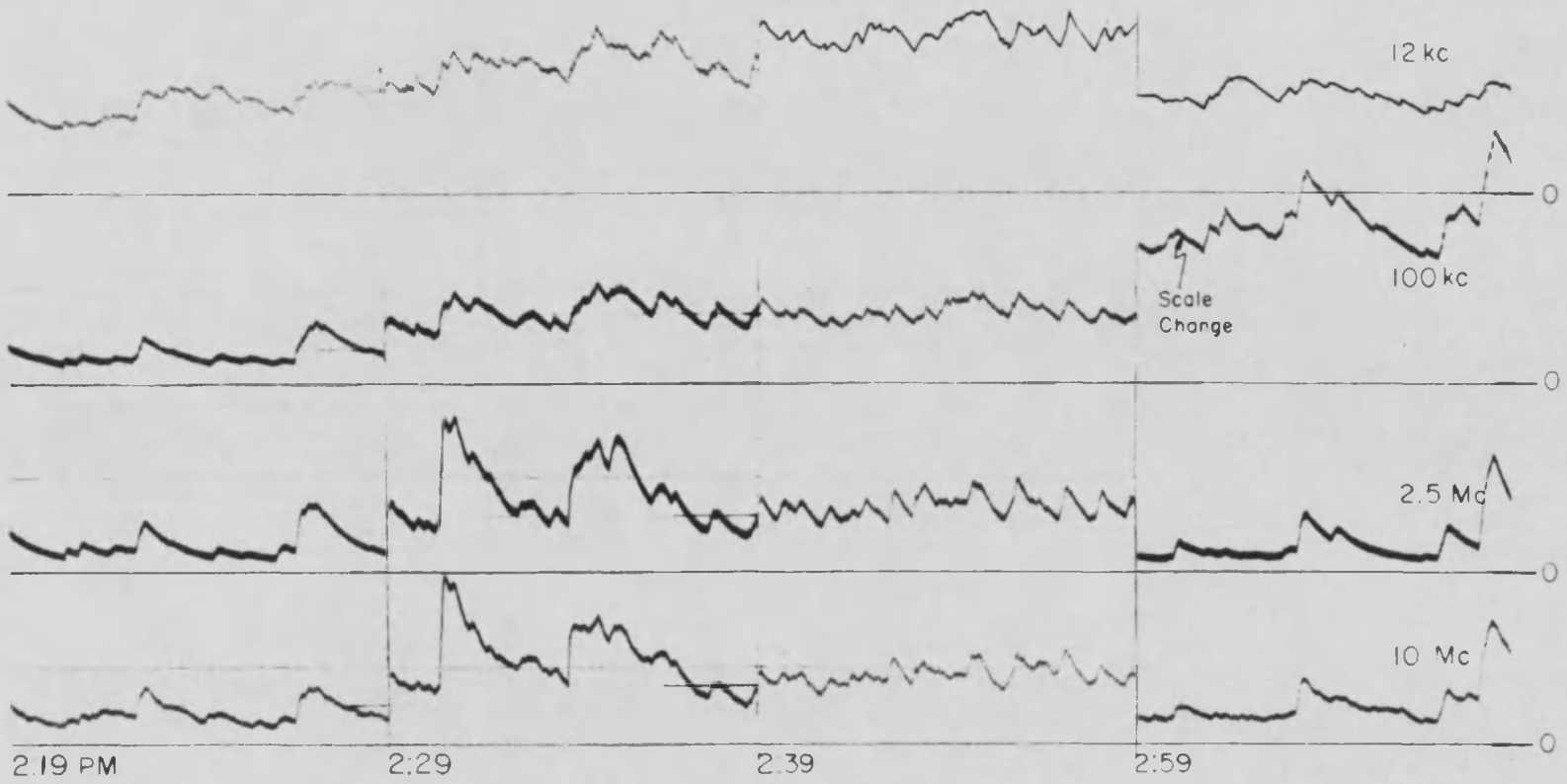

Fig. 4.3 Composite of Sections of Noise Recording for Storm B (August 27, 1964)

the larger pulses on top of this. All of the noise records displayed both types of structures.

4.3 Interesting Sideline - Pulsed Discharges

A brief amount of time was spent looking at pulses which appeared on all channels during times of excessive negative potential gradient (-10,000 v/m or less). Figure 4.4 shows some typical examples of the pulse trains as detected on the lower four frequency channels and recorded on tape through the audio output of the 2.5 and 10 Mc receivers. The source of these pulses is believed to be a type of point discharge from the vertical antennas since a receiver with a loop antenna placed 300 feet from the nearest vertical antenna did not pick up the pulses. The pulsed nature of the discharge is probably due to the periodic build-up and dispersion of space charge in the vicinity of the point of the antenna as discussed by Chalmers[15] and investigated by Trichel[16], Large[4] and others. However, Trichel showed that the pulsed nature is very regular when the point is negative, but in this case regularity was obtained with a positive point. Figure 4.5a shows a pulse pattern observed on several occasions where a distant cloud discharge occurred making the potential gradient more negative. This nearly sinusoidal oscillation reduced in frequency to its previous pulse repetition rate as the field recovered and became less negative. Figure 4.5b shows an odd pulse form which was heard on all channels during a period of intense negative potential gradient.

Monitoring the point discharge with an oscilloscope on September 9, 1964, the following pattern was observed. The point discharge starts with approximately a 60 millisecond period and then advances to

a higher frequency with a period of 5 milliseconds. When the average period becomes less than 5 ms a ground discharge usually occurs, and the point discharge vanishes. However, within several seconds it starts again with approximately a 60 ms period, rapidly advances to a 10 or 12 ms period, then slowly advances to a 5 ms period and the cycle is repeated. This process is recurrent until the potential gradient raises above -10,000 v/m.

No equipment was on hand to correlate pulse frequency with potential gradient or to measure the discharge currents. This observation is quoted as an interesting sideline. For the noise measurement process it was an unwanted phenomenon since during periods of intense negative potential gradient the noise records were rendered useless due to the stronger signals from the point discharge.

All of the following pre-stroke radiation data was obtained during periods of moderate positive potential gradient, so that the records are not distorted by corona or point discharge from the antenna.

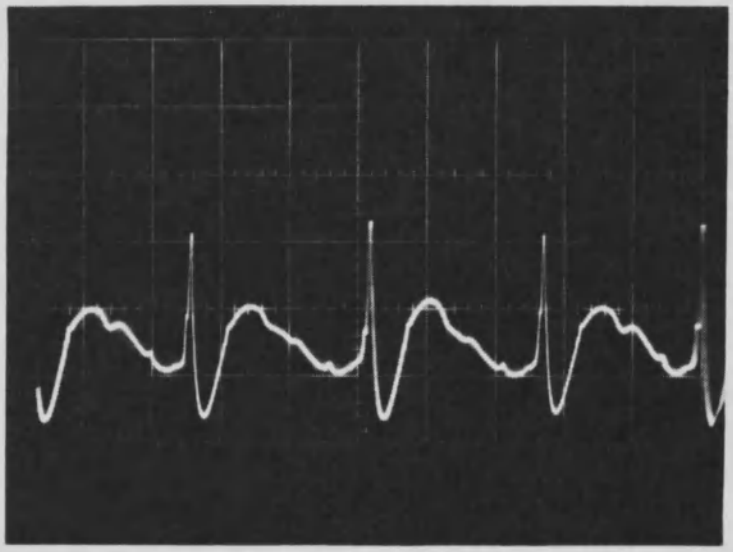

(a)

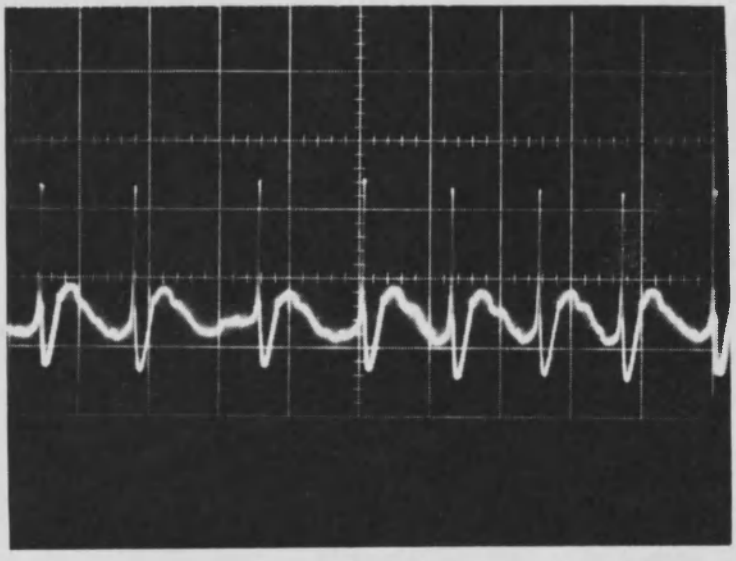

(b)

Fig. 4.4 Periodic Point Discharge Patterns. (a) Recorded on 2.5 Mc at 5 ms/cm, (b) Recorded on 10 Mc at 10 ms/cm.

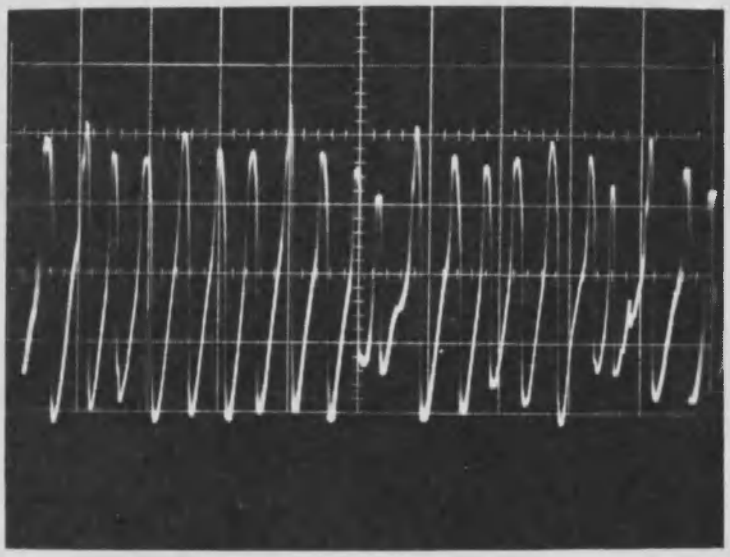

(a)

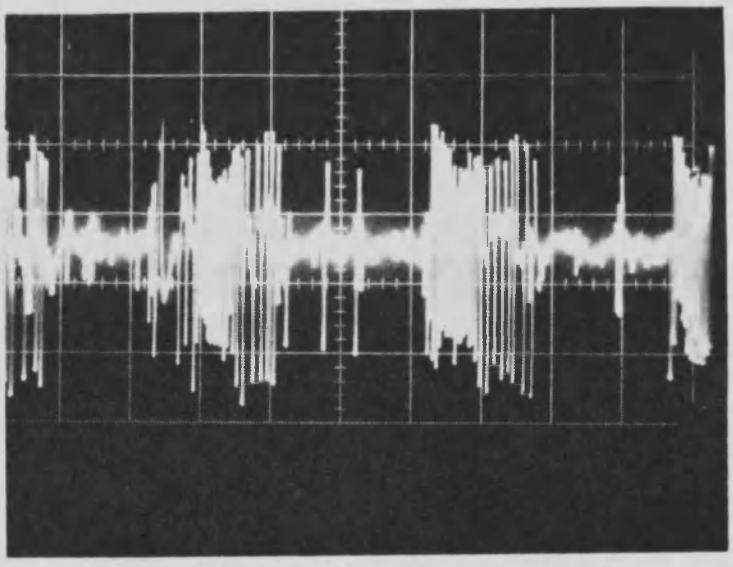

(b)

Fig. 4.5 Point Discharge Patterns. (a) Recorded on 2.5 Mc at 5 ms/cm. (b) Recorded on 2.5 at 20 ms/cm.

Chapter 5

RESULTS AND CONCLUSIONS

5.1 Pre-Stroke Radiation

Figures 5.1 and 5.2 are plots of the noise voltage versus time for storm A and storm B during the period in which the single active storm cell was observed. Using the 10 Mc channel as a reference, notice that for storm B the pre-stroke radiation was initially observed building up approximately 10 minutes before the first ground stroke, and for storm A the noise was initially observed approximately 15 minutes before the beginning of stroke activity.

Workman and Reynolds[17] found in their radar investigations of thunderstorm cell growth that the time interval between the initial radar return (a return from hydrometeors in the vertical convection column) and the initial electrical activity, as indicated by the appearance of lightning, was approximately 12 minutes. Barring coincidence, the correlation of the time interval between the initial noise pickup and the cloud discharges with the time interval between the radar return and cloud discharges might tend to indicate that thundercloud electrification, and therefore noise radiation, is almost simultaneous with the formation of hydrometeors. The element of coincidence will have to be removed by further experimentation.

Figure 5.3 is a plot of noise voltage versus time for August 26, 1964, between 11:20 AM and 12:20 PM (storm C). The recording apparatus was running unattended during this period, but it is included here since

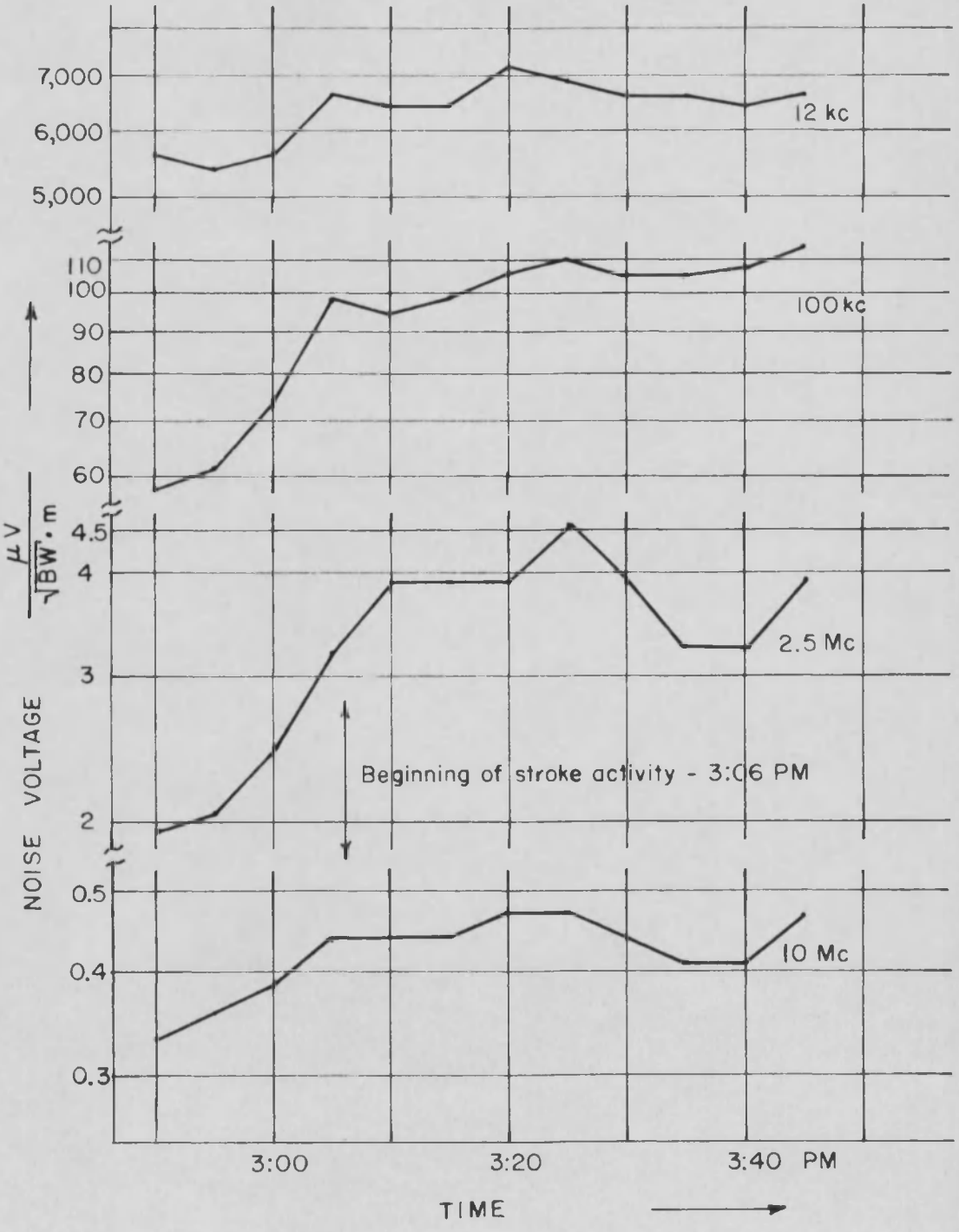

Fig. 5.1 Noise Voltage Versus Time for Storm A.

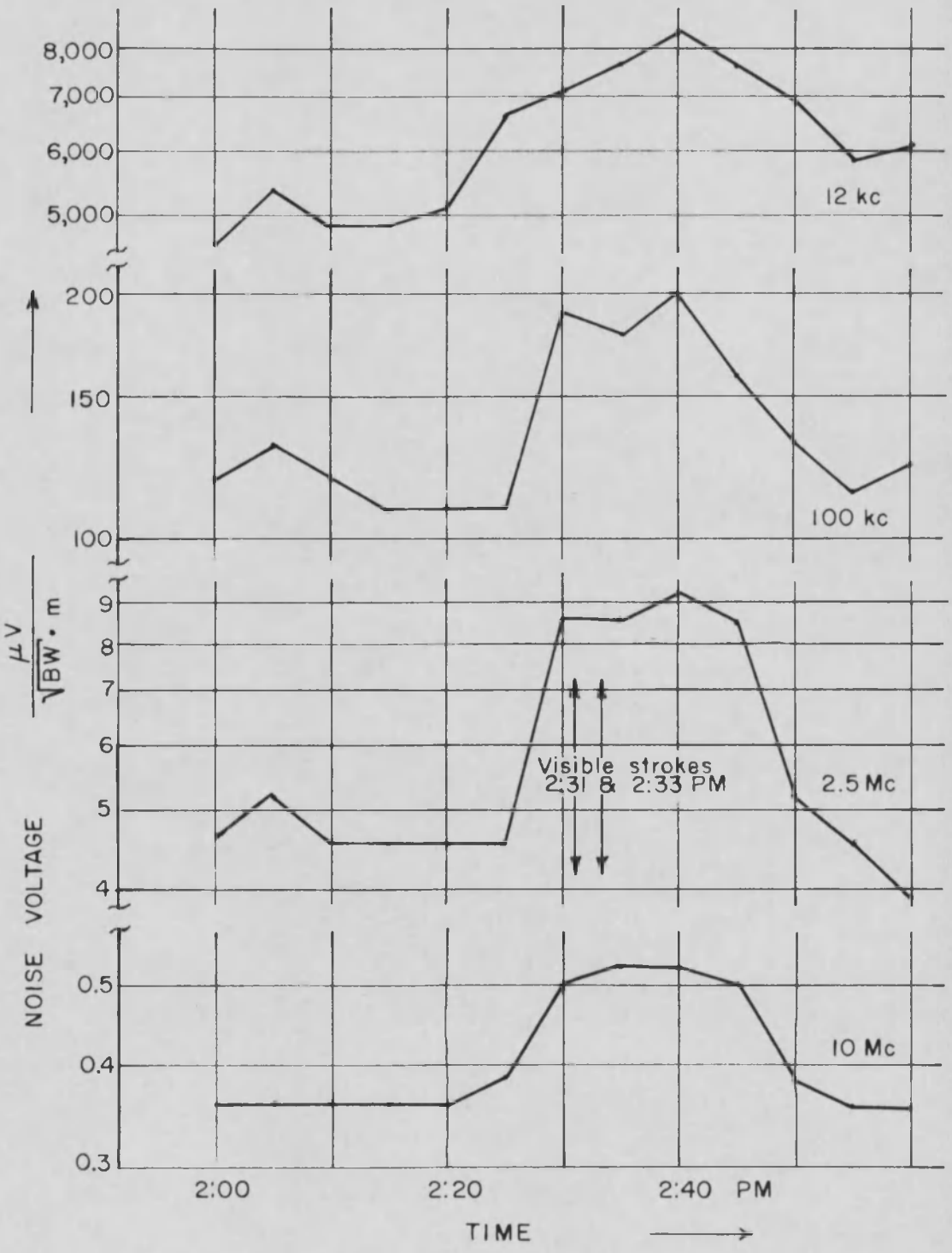

Fig. 5.2 Noise Voltage Versus Time for Storm B.

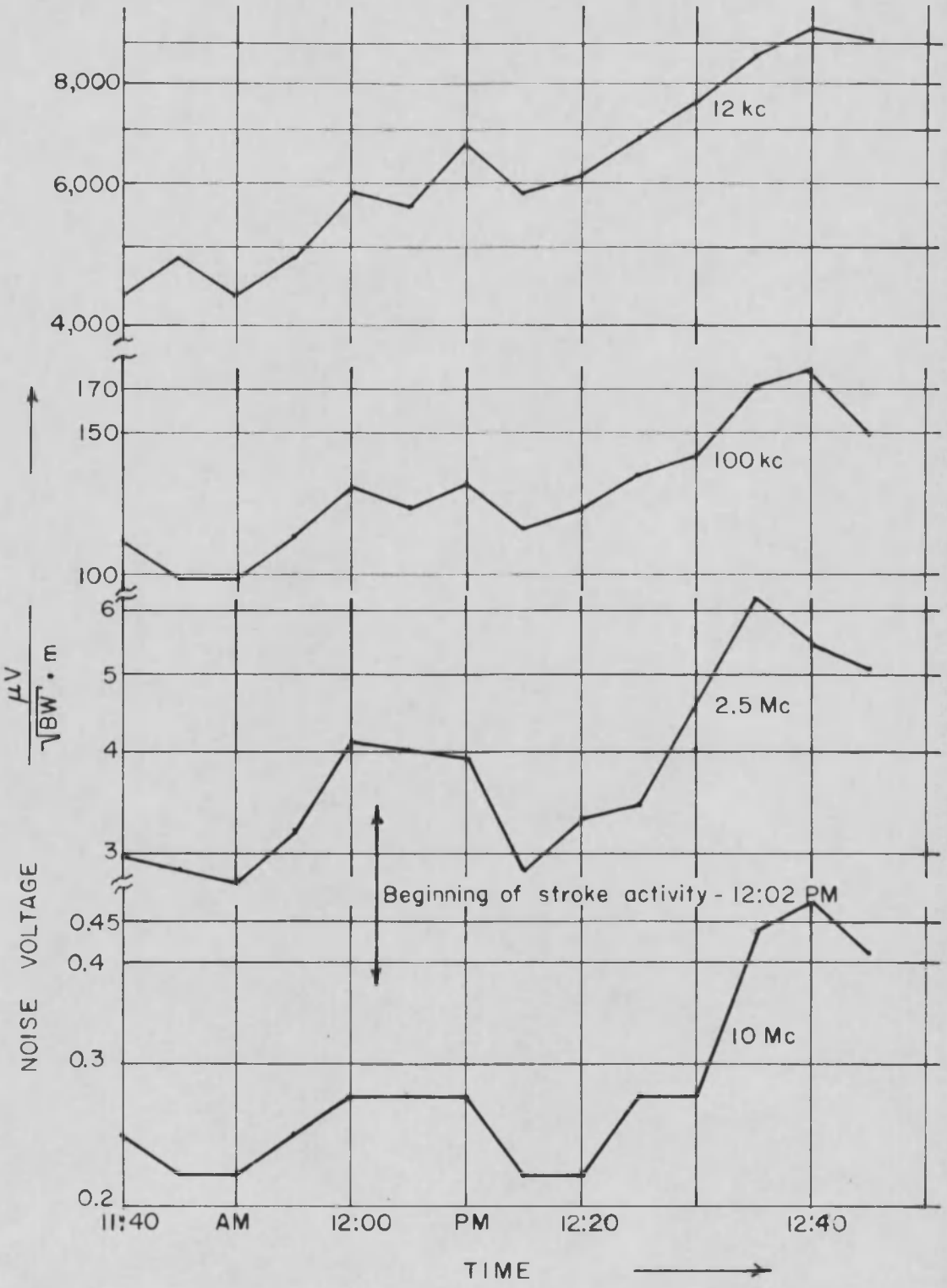

Fig. 5.3 Noise Voltage Versus Time for Storm C.

information extracted from the noise voltage recordings and the field mill records fits in with the general trend as established by storms A and B. The storm cell was initially observed 20 miles northeast of the site at 11:20 AM. This cell apparently moved toward the site during the recording period to give the noise plot as shown. If the data is interpreted correctly, pre-stroke radiation started about 12 minutes before the discharge activity began.

5.2 Radiation as a Function of Frequency

Figure 5.4 is a plot of noise voltage versus frequency for storms A and B. The noise voltage values for storm A were taken at 3:05 PM, approximately one minute before the discharge activity began. For storm B, the noise voltages were taken at 2:30 PM, or 1.5 minutes before the first ground stroke was observed.

This figure may be compared with Fig. 5.5 where the noise voltage was taken before the pre-stroke radiation was evident. One will notice that the slope of the curves for before and during pre-stroke radiation are almost identical and in both cases the radiation drops off approximately as $f^{-1.2}$. Therefore, if one assumes that the background noise prior to pre-stroke radiation is due only to lightning strokes from distant storms (i.e. distant enough that pre-stroke radiation is not detectable yet close enough that the various propagation effects are negligible), one could venture that the noise generated within a cloud is of the same nature as that generated from a lightning stroke--at least in the frequency range from 100 kc up to 10 Mc and perhaps to 100 Mc. However, one would have to investigate the fine characteristics of both types of noise to be certain of this.

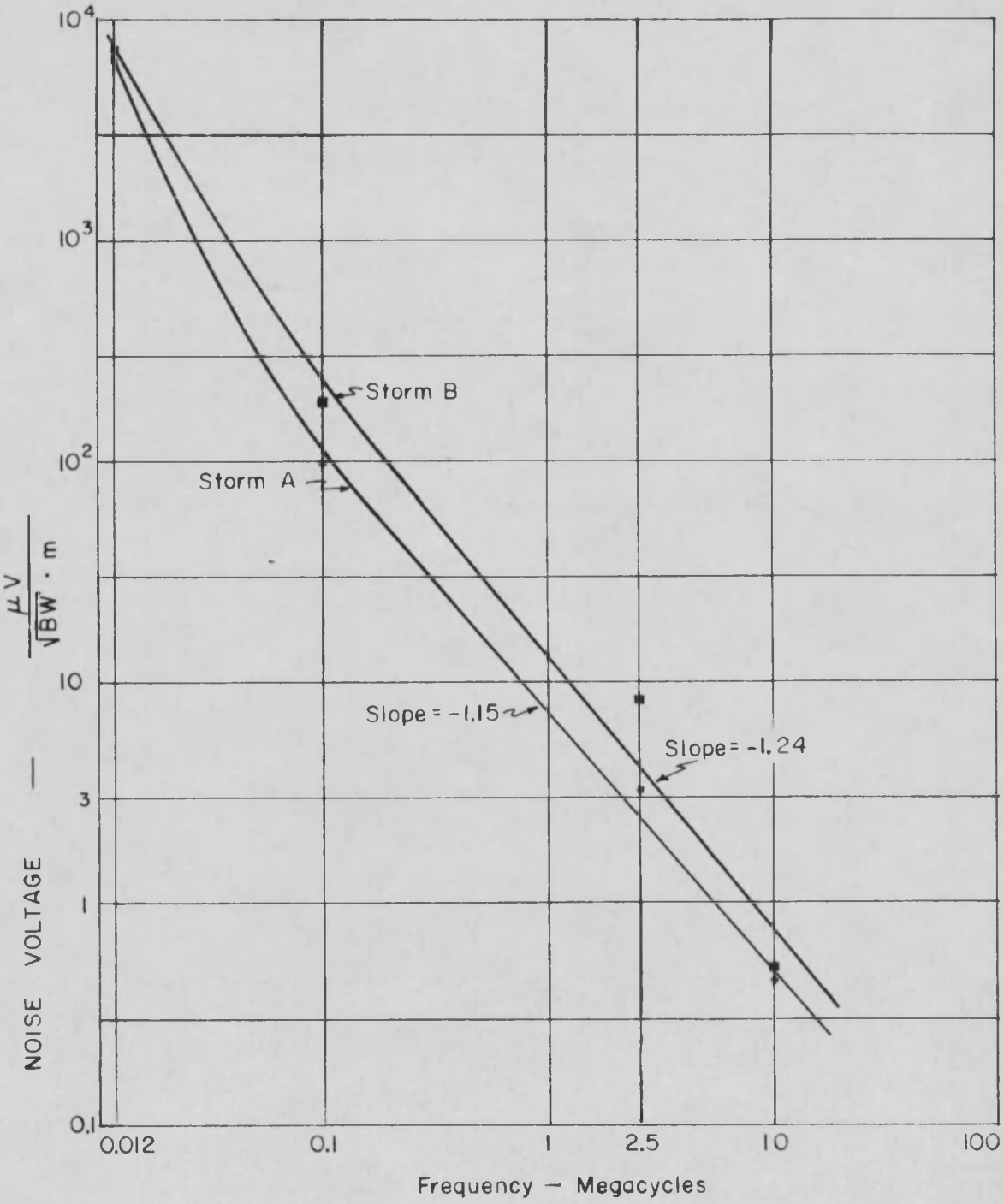

Fig. 5.4 Noise Voltage During Pre-Stroke Radiation Versus Frequency for Storms A and B.

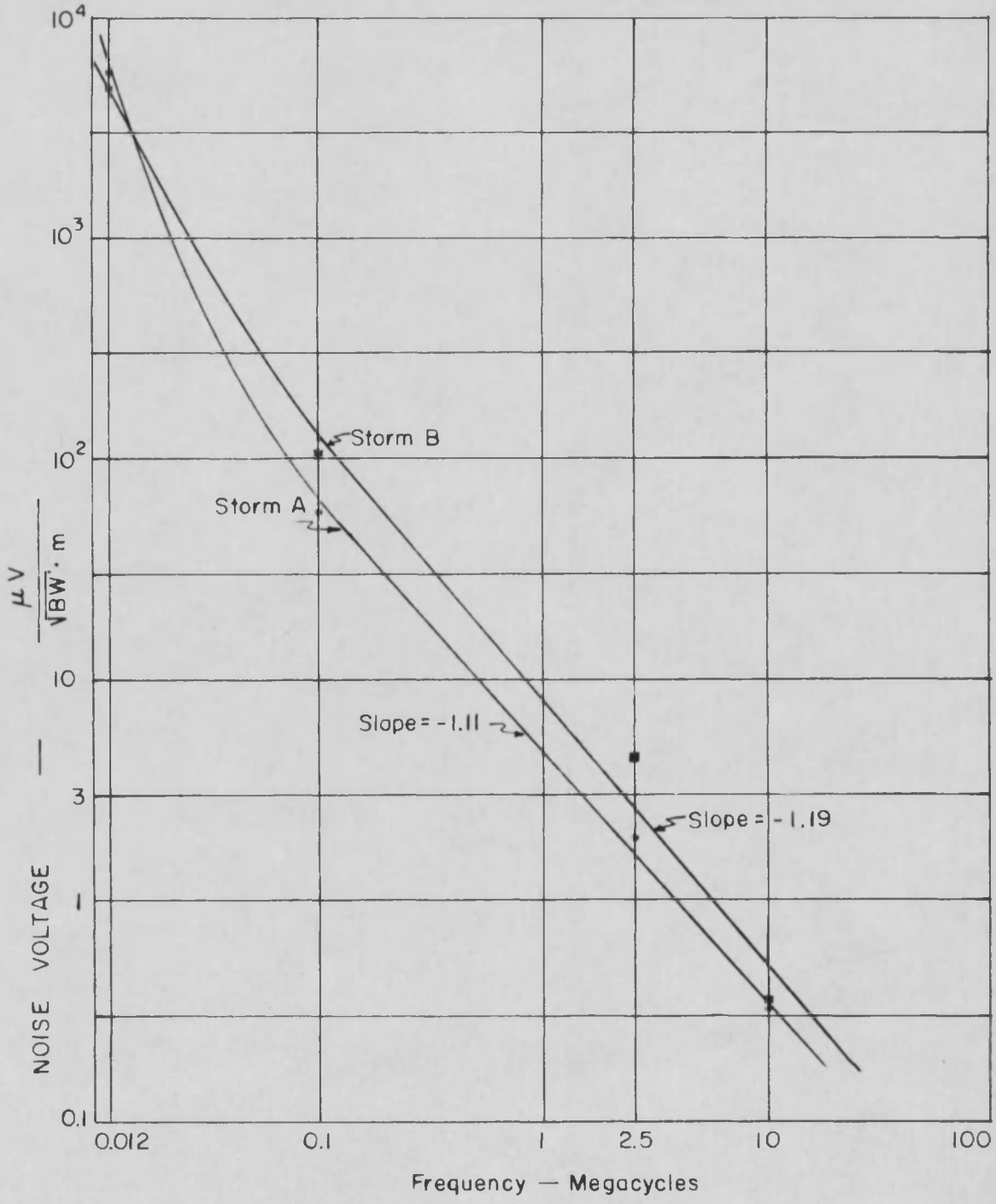

Fig. 5.5 Noise Voltage Prior to Pre-Stroke Radiation Versus Frequency for Storms A and B.

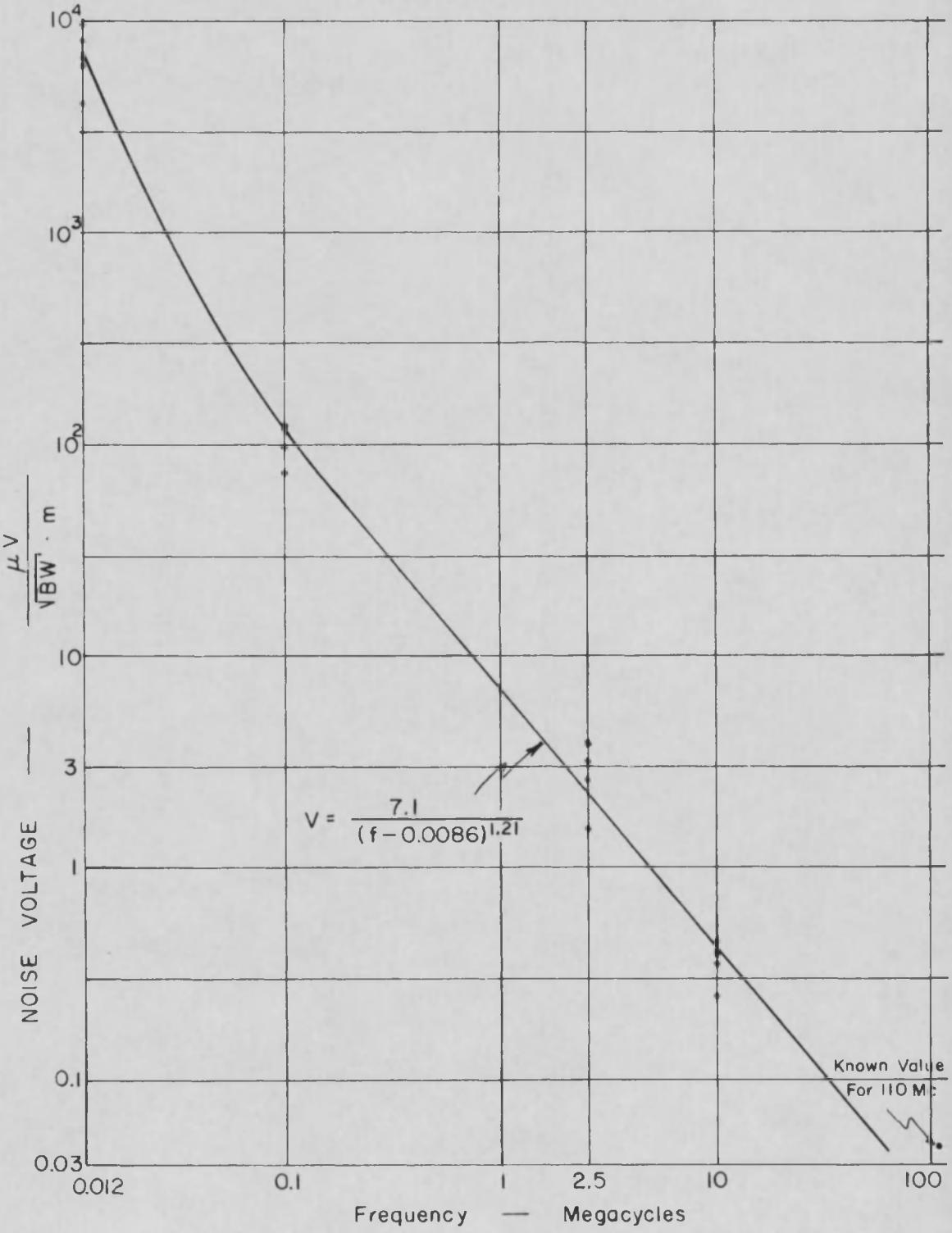

Fig. 5.6 Noise Voltage Versus Frequency for Five Data days at 3:00 PM.

Figure 5.6 is a plot of the noise voltage versus frequency for five days at 3:00 PM. The value of the noise voltage shown for 110 Mc was calculated using the minimum sensitivity of the receiver since the noise fluctuations were known at times to attain at least this value. The equation of the curve for a good fit was computed by the method of least squares and by iteration and found to be

$$V = \frac{7.1}{(f - 0.0086)^{1.21}}$$

where V is the noise voltage in microvolts x (bandwidth in kc)$^{-1/2}$ x (meter)$^{-1}$, and f is the frequency in megacycles.

The difference in smoothing filter time constants between the kilocycle channels and the megacycle channels was investigated and found to have no appreciable effect on the average noise measurements as analyzed and compared here.

For general interest, a plot of noise voltage versus frequency for six days at three different times is given in Fig. 5.7 with tabulations in Table 5.1. One will notice that all of these noise plots are similar in form and have approximately the same slope from 100 kc to 10 Mc.

5.3 Summary

From this experiment it is deduced that in the frequency range investigated there is appreciable pre-stroke radiation; the radiated noise voltage is approximately a function of $(f)^{-1.2}$; the noise generation appears to be related to the vertical convection channel in a thundercloud and may possibly be derived from inter-cloud corona or sources similar to radiation from lightning strokes.

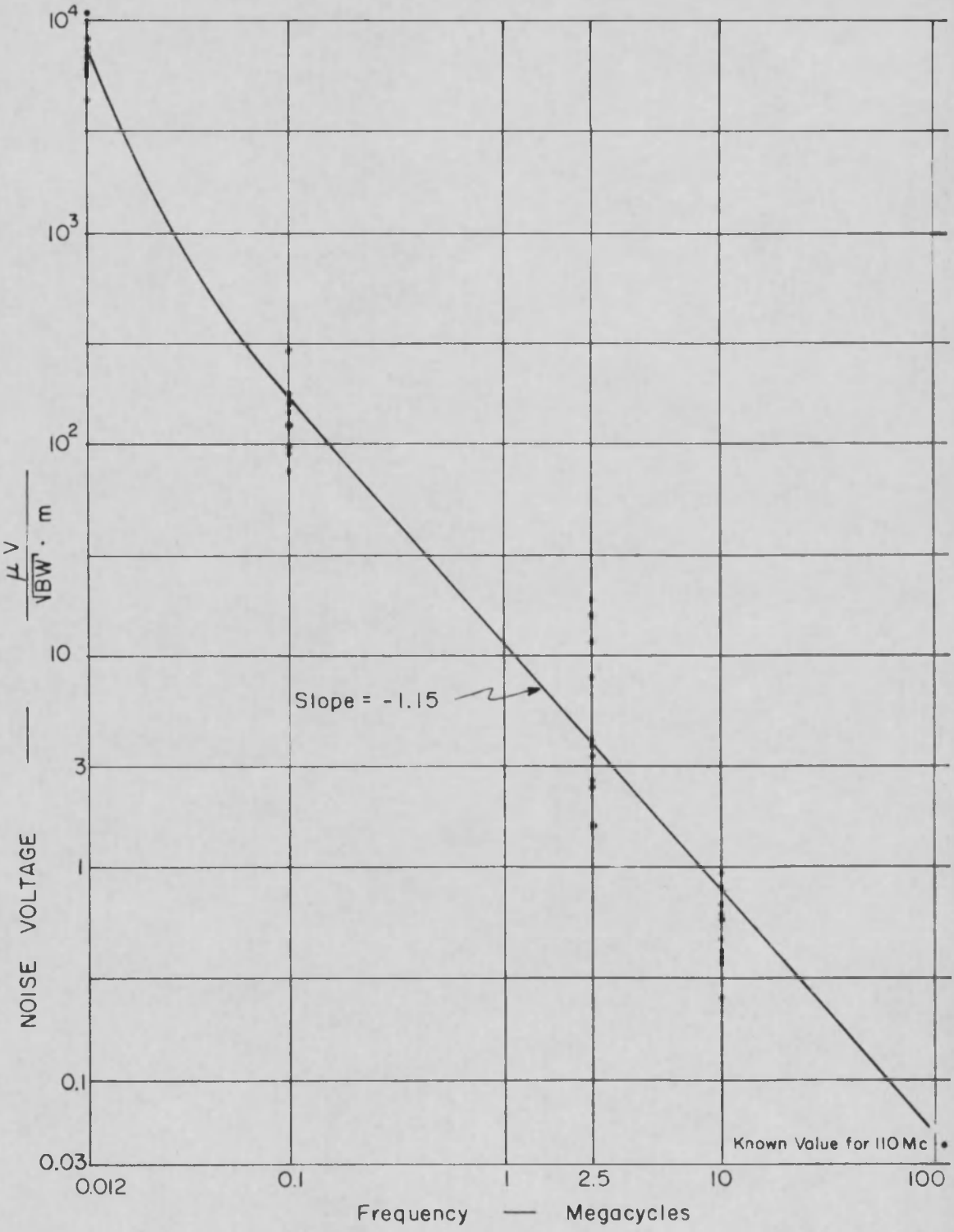

Fig. 5.7 Noise Voltage Versus Frequency for Six Data Days at Three Different Times.

Table 5.1 Tabulation of Noise Voltages for Fig. 5.7

Date 1964	Time PM	Noise 12 kc	Voltage 100 kc	Noise Voltage in $\frac{\mu V}{\sqrt{BW} \cdot m}$ 2.5 Mc	10 Mc
August 16	5:00	7,380	123	3.31	0.469
	7:10	6,110	283	18.5	0.579
August 17	3:00	9,600	123	3.91	0.413
	4:50	11,300	154	11.69	0.964
August 20	3:00	4,100	90	1.52	0.248
	5:00	5,860	94	2.59	0.689
	7:00	6,620	144	7.79	0.827
August 24	3:00	5,610	74	2.43	0.385
August 25	3:00	8,130	126	2.65	0.385
	7:00	7,380	176	15.80	0.607
August 27	3:00	6,110	123	3.89	0.358

5.4 Further Studies

Additional experimentation is planned at higher frequencies and with directional antennas. The difficulty of isolating a single storm cell in the present work has demonstrated the need for a directional array. This will not only help by isolating storm cells, but will also give a better measure of the beginning of pre-stroke radiation from clouds. The first part of pre-stroke radiation may have been masked out by surrounding storms, since omni-directional antennas were used in the work reported here.

It is planned to monitor 110 Mc in the summer of 1965 with a quad-yagi array in an effort to begin where this work was terminated. 110 Mc is chosen, since it is definitely known that radiation from lightning strokes is detectable at this frequency. If results are positive here, one would like to investigate higher frequencies where a manageable storm tracking system could be fabricated.

5.5 Conclusions

The results of this work are apparently positive inasmuch as storm cell movement and build-up is detectable with omni-directional antennas. However, the minimum detectable radio frequency noise emission could be improved by utilizing directional arrays.

No definite information was obtained on the exact source of the noise, but local discharges seem most probable.

If, in further work, appreciable radiation is found in the very high frequency to ultra high frequency range a passive storm tracking radar could probably be fabricated and utilized in tracking storm cells and predicting visible electrical activity.

REFERENCE

1. Jansky, Karl G., Directional Studies of Atmospherics at High Frequencies, Proc. IRE, 20(12) 1920-1932, 1932.

2. Sartor, J. Doyne, Radio Emission from Clouds, J. Geophys. Res., 68(18), 5169-5172, 1962.

3. Hogg, D. C., and R. A. Semplak, The Effect of Rain and Water Vapor on Sky Noise at Centimeter Wavelengths, Bell System Tech. J., 40(5), 1331-1348, 1961.

4. Large, M. I., The Radio Interference Produced by Corona Discharge, J. Appl. Phys., 10, 245-250, 1957.

5. Sayers, D. P., Forrest, J. S., and F. J. Lane, 275-kv Developments on the British Grid System, J. Instn. Elect. Engrs., 99(II), 590-595, 1952.

6. Aiya, S. V. C., Noise Power Radiated by Tropical Thunderstorms, Proc. IRE, 43(8), 966-974, 1955.

7. Aiya, S. V. C., Noise Radiation from Tropical Thunderstorms in the Standard Broadcast Band, Nature, 178(4544), 1249, 1956.

8. Horner, F., Narrow-band Atmospherics from two Local Thunderstorms, J. Atmospheric Terrest. Phys., 21(1), 13-25, 1961.

9. Hill, E. L., Electromagnetic Radiation from Lightning Strokes, J. Franklin Inst., 263(2), 107-119, 1957.

10. Arnold, Helen R., and E. T. Pierce, Leader and Junction Processes in the Lightning Discharge as a Source of VLF Atmospherics, J. Res. NBS/USNC-URSI, 68D(7), 771-776, 1964.

11. Dennis, A. S., and E. T. Pierce, The Return Stroke of the Lightning Flash to Earth as a Source of VLF Atmospherics, J. Res. NBS/USNC-URSI, 68D(7), 777-794, 1964.

12. Pierce, E. T., Meteorological Aspects of the Sources of Atmospheric Noise in Lightning, Paper in Radio Noise of Terrestrial Origin, ed. F. Horner, Elsevier, 55-71, 1962.

13. Landon, V. D., A Study of the Characteristics of Noise, Proc. IRE, 24(11), 1514-1521, 1936.

14. Jansky, Karl G., An Experimental Investigation of the Characteristics of Certain Types of Noise, Proc. IRE, 27(12), 763-768, 1939.

15. Chalmers, J. A., Atmospheric Electricity, Pergamon Press, 1957.

16. Trichel, G. W., The Mechanism of the Negative Point to Plane Corona Near Onset, Phys. Rev., 54, 1078-1084, 1938.

17. Workman, E. J., and S. E. Reynolds, Electrical Activity as Related to Thunderstorm Cell Growth, Bull. Amer. Met. Soc., 30(4), 142-144, 1949.